Morphology transition observed in a phase separating fluid

F. Perrot,[1] D. Beysens,[2] Y. Garrabos,[3] T. Fröhlich,[1] P. Guenoun,[1]
M. Bonetti,[1] and P. Bravais[4]
[1]*Service de Physique de l'Etat Condensé, CEA Saclay, F-91191 Gif-sur-Yvette Cedex, France*
[2]*Département de Recherche Fondamentale sur la Matière Condensée, CEA Grenoble, F-38054 Grenoble Cedex, France*
[3]*Institut de Chimie de la Matière Condensée de Bordeaux, CNRS, Université Bordeaux I, F-33608 Pessac, France*
[4]*L'Air Liquide, F-38360 Sassenage, France*
(Received 6 October 1998)

The relation between morphology and kinetics of phase ordering in fluids is studied near a critical point (with benefit of universality) and under reduced gravity. The volume fraction ϕ of the phases governs the phase ordering. It is varied in a SF_6 sample (density 0.85% off critical) by performing thermal quenches below the coexistence curve (range: 50–2490 μK). We observe for $\phi_H=(29\pm3)\%$ a transition from a pattern of isolated drops ($\phi<\phi_H$), whose distance grows as $(\text{time})^{1/3}$, to a pattern of interconnected drops ($\phi>\phi_H$), with distance growing as $(\text{time})^1$. The transition separates the regions where collisions of droplets, which dominate the dynamics, are due to Brownian diffusion or to hydrodynamic interactions. [S1063-651X(99)12502-9]

PACS number(s): 64.70.Fx, 64.60.Qb, 05.70.Jk, 81.70.Ha

I. INTRODUCTION

A general goal in physical, chemical, and life sciences aims at understanding the connection between the growth and the morphology of developing patterns. A general process in interacting domains is fusion or coalescence, which we address more particularly in this study. Several mechanisms are involved in bringing the droplets into contact, Brownian diffusion [1,2] or internal and external hydrodynamics flows [3]. To address the above question, the neighborhood of a critical point is particularly appealing. After a thermal quench below the coexistence curve, droplets of gas and liquid nucleate and grow under typical patterns [4]. We are interested in the late stages of growth when phase boundaries are already well developed and the concentrations of the phases are very close to the equilibrium values, as defined by the coexistence curve (Fig. 1). Then the drops grow just because the system tends to minimize the total surface separating the phases (e.g., by coalescence events). In the vicinity of the critical point, one benefits from the universality features of scaling. Scaling by proper units of length and time implies that all data from different experiments and different systems can be cast on the same universal master curves. In addition, the growth kinetics is slowed down (this is the well-known ''critical slowing down'' [5]), which enables phase separation to be studied for a longer time, making the experimental study easier. Excellent temperature stabilization is needed, and gravity effects have to be suppressed.

The order parameter of a pure fluid is defined as the normalized density difference $M=(\rho-\rho_c)/\rho_c$, with ρ_c the critical density. At the gas-liquid critical point, the isothermal compressibility diverges and the thermal diffusivity goes to zero. The natural length scale is the correlation length ξ of the order parameter fluctuations, which varies with temperature T as $\xi=\xi_0(1-T/T_c)^{-\nu}$, with T the temperature and T_c the critical temperature, ξ_0 a nonuniversal amplitude, and $\nu=0.63$ the universal critical exponent. The natural time scale is the relaxation time of the order parameter fluctuations of size ξ, given by $t_\xi=6\pi\eta\xi^3/k_BT$, with η the shear viscosity and k_B the Boltzmann constant [5]. We consider all critical amplitudes below T_c.

II. BACKGROUND

A typical phase-separation experiment consists in quenching a sample from an initial state (M, temperature T_i) where it is homogeneous, to another state (M, temperature T_f) where it is no longer stable and where the process of phase separation occurs. The equilibrium volume fraction ϕ of the minority phase is related to T_c, the coexistence temperature T_{cx}, and the quench depth $\delta T=T_{cx}-T_f$ by (Fig. 1)

$$\phi=\frac{M^+-M}{M^+-M^-}=\frac{1}{2}\left[1-\left(1+\frac{\delta T}{\Delta T}\right)^{-\beta}\right]. \tag{1}$$

Here $\beta=0.325$ is a universal exponent and $\Delta T=T_c-T_{cx}$ is calculated from the coexistence curve expression $M=\pm B(1-T/T_c)^\beta$ where B is system dependent [6].

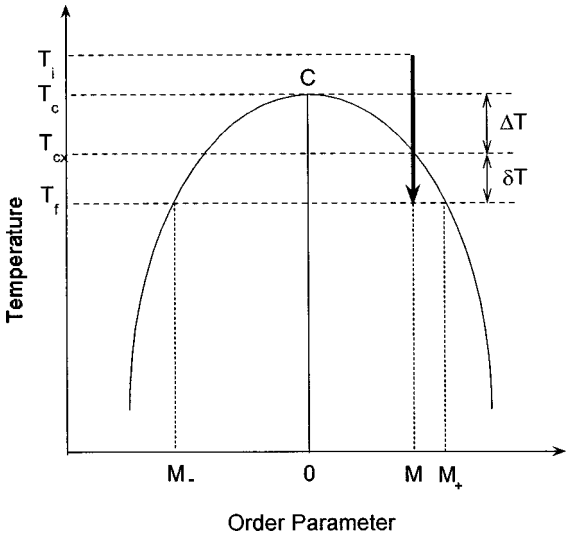

FIG. 1. Schematic phase diagram for simple fluids and liquid mixtures. T is temperature and M is the order parameter [$M=(\rho/\rho_c)-1$ for simple fluids and $M=c-c_c$ for liquid mixtures].

Phase separation at $M=0$ ($\phi=\frac{1}{2}$) has been extensively studied [7], and mainly with liquid mixtures [8]. After a thermal quench at T_f into an unstable state, the two growing phases of equal volume form an interconnected pattern of domains that continuously coalesce. A number of experiments [9] under reduced gravity with a near density-matched binary mixture of partially deuterated cyclohexane and methanol (C^*M) and pure fluids CO_2 and SF_6 have already been carried out. Results show that the influence of convective flows and sedimentation can be efficiently removed. A characteristic length L_m of the domains can be defined as the pseudoperiod between the phases. At late times, $L_m \sim t$. When expressed in the scaled units, $K_m^*=2\pi\xi/L_m$ and $t^*=t/t_\xi$, all the results obtained with liquids and fluids at different quench depths can be cast on the same master curve, thus demonstrating scaling and universality in the sense of phase separation. The curve can be described by the phenomenological equation given by Furukawa [10]:

$$(K_m^{*-1}-1)-[(A^*/B^*)^{1/2}\{\tan^{-1}[K_m^{*-1}(B^*/A^*)^{1/2}] - \tan^{-1}[(B^*/A^*)^{1/2}]\}]=B^*t^*, \quad (2)$$

where A^* and B^* are two adjustable parameters. For binary liquids [8], $A^*=0.14\pm0.01$ and $B^*=0.022\pm0.001$. We call this evolution, characterized by an interconnected morphology and a fast growth, ''fast interconnected.''

Only a few experimental results are available when the order parameter is systematically varied from $M=0$ [11–13]. When the volume fraction is somewhat lower than 0.5, the drops collide and coalesce but stay disconnected. A number of results obtained either with the above density-matched binary liquid C^*M under a weak density gradient, which enables the order parameter to be varied in the sample [12], or with C^*M and pure fluid SF_6 under reduced gravity [14], shows that phase separation in such conditions is characterized by a pattern of monodisperse tightly packed droplets of the minority phase whose growth can be expressed over more than seven decades in time by a single reduced law with exponent $\frac{1}{3}$:

$$K_m^* \approx 0.9 t^{*1/3}. \quad (3)$$

All the above experiments show that $K_m^* \approx 1$ when $t^* \approx 1$, which means that nucleation proceeds from fluctuations of the size of the correlation length, in agreement with the concept of ''generalized nucleation'' [1]. We call this evolution, characterized by a disconnected morphology and a slow growth, ''slow disconnected.''

When the volume fraction is very small ($\phi<0.03$), the droplets do not coalesce and grow by a mechanism of diffusion through the majority phase. Experiments [13] show that, although the initial growth follows a power law with time whose exponent $\frac{1}{2}$ or $\frac{1}{3}$ depends on the initial supersaturation, the late stages are always characterized by a $\frac{1}{3}$ growth law exponent as described by Lifshitz and Slyozov [15].

These previous works [12,14] are in support of universality for phase ordering in fluids and in liquid mixtures. Although the parameter which determines either behavior is suspected to be the equilibrium volume fraction ϕ of the minority phase, this conclusion does not clearly follow from the experiment. The above experiment only shows that the disconnected-interconnected transition holds for $c-c_c>0.01$ (binary liquid mixtures) and $(\rho/\rho_c)-1>1\%$ (simple fluid).

In this study we show that modifying the volume fraction by varying the quench depth in the same homogeneous sample enables morphology and kinetics to be changed. We thus emphasize the key role of volume fraction and determine a value ($29\pm3\%$) for the threshold volume fraction value ϕ_H which delimits the two morphology and growth regions. For this purpose, we performed minute thermal quenches in a slightly off-critical sample of SF_6 for which ϕ can be varied according to the quench depth. A pure fluid was used, because its dynamics remains fast enough so that local equilibrium of the phases can be reached, even very close to T_c, within an equilibration time compatible with an experiment time. In addition, the density of such fluids can be accurately measured by the variation of the meniscus height [16]. Since the gravity effects are very pronounced under the earth gravity field the experiments were performed under reduced gravity [17]. Note that, although the thermal diffusivity of pure fluids goes to zero at the critical temperature T_c, another mechanism of heat transport by pressure mode, the so-called ''piston effect,'' becomes very efficient near T_c due to the large compressibility of the fluid, thereby allowing thermalization to be limited only by the thermal response of the thermostat [18].

III. EXPERIMENT

The experiment is carried out with pure fluid SF_6 in the Critical Point Facility of European Space Agency [19]. The fluid is enclosed in a CuBe rectangular shaped cell with two windows. The internal volume is a cylinder (12 mm internal diameter, 3 mm thickness), with two natural sapphire windows (12 mm external diameter) epoxied using their cylindrical surface to the CuBe wall. The cell is filled with an accuracy of order 0.05% with SF_6 (L'Air Liquide, of quality better than 99.980%). This density is off critical by 0.85% from the critical density as checked by the variation of the meniscus height with temperature [16]. The coexistence temperature T_{cx} is shifted from T_c by $T_c-T_{cx}=30\,\mu$K. It is the nonwetting minority phase (vapor) which nucleates.

The cell is set in a high precision thermostat having a temperature stability of within 20 μK and a minimum temperature stepping of 100 μK. The temperature in the fluid can be analyzed by considering the light transmittency as a temperature probe in the sample. Temperature quenches are performed at a mean rate of 200 μK/s and last approximately 5 s. In all the quenches analyzed here, the sample temperature begins to vary approximately 8 s after the set point was changed, T_c is crossed 4 s later, and the experiments are analyzed 8 s later on (i.e., 20 s after the set point). We consider the time where the sample crossed T_c as the time of origin.

The cell is illuminated by a parallel white light beam. A plane of order 0.1 mm fluid thickness is imaged on a charge coupled device (CCD) video camera and a photographic camera. Laser light scattering measurements (turbidity, light scattered at 22° and 90° angle) are used to determine the coexistence temperature T_{cx}. The transition temperature of SF_6 was checked during the flight after homogenization at $T_{cx}+1$ K for one hour. The temperature which was found

($T_{cx}=45.532\,60\,°C$) is the same as 18 months earlier within 1 mK.

Remote control is used to command the experiment in real time from the ground. A directed acceleration of order 10^{-6} times the earth gravity, originating from the friction with the high atmosphere and from the fact that the setup is not located at the center of mass of the spacecraft, is permanently applied to the samples. Moreover, an acceleration (g jitter) which is randomly oriented is also present. It is generally lower than $10^{-4}g$, a value which can increase depending on the spacecraft activity. We did not notice any correlation between the residual accelerations and the phase separation process as it is analyzed below.

Four quenches were performed: quench 1, from $T_{cx}+260\,\mu$K to $T_{cx}-1.81$ mK ($\phi=0.37$); quench 2, from $T_{cx}+1.55$ mK to $T_{cx}-2.49$ mK ($\phi=0.38$); quench 3, from $T_{cx}+1.66$ mK to $T_{cx}-430\,\mu$K ($\phi=0.29$); quench 4, from $T_{cx}+50\,\mu$K to $T_{cx}-50\,\mu$K ($\phi=0.14$).

IV. EXPERIMENTAL RESULTS AND DISCUSSION

The spacing L_m is measured directly on the video or photo pictures by averaging over nearest-neighbor pairs of droplets. This procedure is repeated over many pairs located at different places in the cell. We observe that the cell is not homogeneous when the initial temperature T_i of the quench is nearer to the coexistence temperature than 1 mK. This happens during quenches 1 and 4. For quench 1, 176 s after the beginning of the quench, the right part of the cell is seen to phase separate earlier than the left part. We attribute this difference in transition temperature to a density gradient across the sample. As the derivative $(\partial\rho/\partial T)_p$ (p is pressure) goes to infinity at the critical point, a minute temperature gradient, as the gradient induced by the very small heat flow necessary to ensure thermal regulation, is able to induce noticeable density gradient. To give an order of magnitude, at 1 mK above T_c, the derivative $\rho^{-1}(\partial\rho/\partial T)_p\approx 6.7\times 10^3\,\mathrm{K}^{-1}$, which means that a 1 μK temperature difference causes a 0.7% difference in relative density. The density gradients in quenches 1 and 4 are directed in the same direction. Its amplitude is difficult to estimate because it depends on the temperature history of the sample. Anyway, data analyzed in the middle of the cell can be related to the average sample density, under the reasonable assumption that the density gradient is symmetrical with respect to the cell symmetry axis. In Fig. 2 are shown the patterns for quench 2 ($\phi=0.38$, interconnected-fast growth) and 4 ($\phi=0.14$, disconnected-slow growth).

The experimental results for the different quench depths are reported in Fig. 3 on the same curve in reduced units $K_m^*=2\pi\xi/L_m$ and $t^*=t/t_\xi$. (The parameters needed to analyze the data are from Ref. [14].) For quenches 1 and 4, where density gradients are present, the data obtained in the middle of the cell correspond to morphology and growth laws different from those near the border wall. We report the data corresponding to both behaviors. The data are compared with the two curves obtained for interconnected morphology and fast growth [Eq. (2)] and disconnected morphology and slow growth [Eq. (3)]. The data fit reasonably well to the slow growth ''universal'' curve. However, the data corresponding to the ''fast'' growth are systematically higher than the curve corresponding to binary liquids. This tendency was

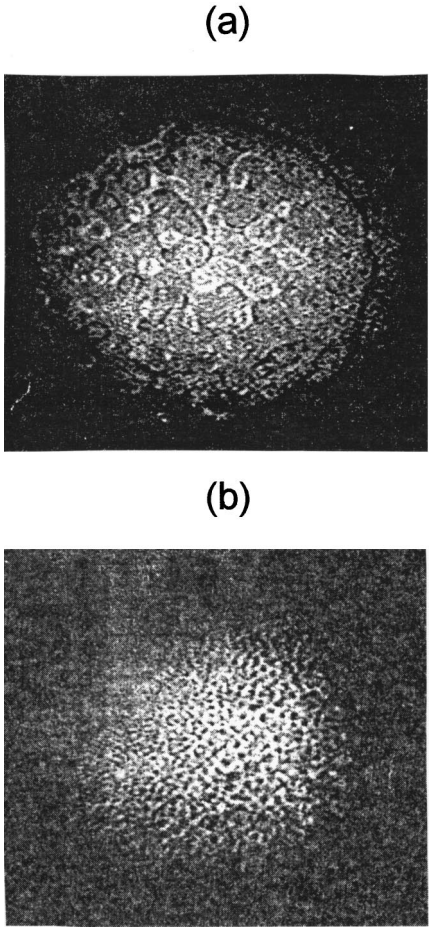

FIG. 2. Video pictures of the phase-separation pattern. (a) Quench 2: $T=T_{cx}-2.49$ mK, $t=22$ s; (b) $T=T_{cx}-50\,\mu$K, $t=1900$ s. The largest dimension of the picture corresponds to 14 mm.

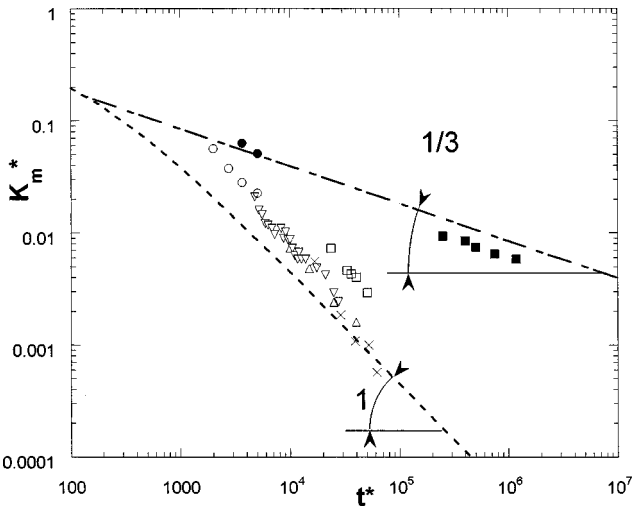

FIG. 3. Growth laws expressed in scaled units K_m^* and t^* (see text). The curves refer to an average of the data obtained in different liquid mixtures. The open dots (lower curve) correspond to the interconnected-fast growth and full dots (upper curve) correspond to the disconnected-slow growth. Because of a density gradient (see text), the data for quenches 1 and 4 are from the middle of the sample and near a wall. (Quench 1: ■, □; quench 2: △; quench 3: ▽; quench 4: ●, ○.) Crosses are from ''fast'' growth in CO_2 (Ref. [9]).

also noticed with one set of data obtained in a 1 mK quench with fluid CO_2 (Fig. 3 and Ref. [9]). We cannot attribute this discrepancy to a wrong estimation of the SF_6 parameters like viscosity, correlation length, etc. It cannot be due, either, to a wrong estimation of the time origin of the evolution process as the time where the data are analyzed is taken much later than the quench time. Since the discrepancy is the same for ''deep'' quenches (no. 1 and no. 2) and ''shallow'' quenches (no. 1 and no. 4), we rather suspect the effect of coupling between the heat transport, due to the extreme compressibility of the fluid (''piston effect'' [18]), and the mass transport of the phase-separation process.

Anyway, these experiments demonstrate that the volume fraction is undoubtedly the important parameter for both morphology and growth laws of a droplet pattern. From the data, we find a disconnected morphology and a slow growth at $\phi=0.14$ and an interconnected morphology and a fast growth at $\phi=0.29$, 0.37, 0.38. These data alone enable a threshold volume fraction $\phi_H=0.22\pm0.07$ to be determined. These results are in agreement with previous experiments with SF_6 where a disconnected morphology and a slow growth were observed for the volume fractions $\phi=0.13$, 0.22, 0.26 [14]. We also report the data of CO_2 [9] where interconnected morphology and fast growth were observed for a density critical within 0.1% and a quench depth of 1.3 mK ($\phi=0.5+0/-0.017$). One also considers the results obtained with the C^*M liquid mixture [14], where a disconnected morphology and a slow growth was observed for a volume fraction $\phi=0.31\pm0.04$. It is interesting to visualize the threshold in volume fraction by reporting all available data in the units $1-T/T_c$ versus M/B (Fig. 4). In a log-log plot, the coexistence curve is represented by a straight line with exponent $1/\beta$, and the threshold $\phi=\phi_H$ between interconnected-fast and disconnected-slow is a line parallel to it. The ''best'' line corresponds to $\phi_H=0.29\pm0.03$ in Fig. 4. Note that the border between interconnected-fast and disconnected-slow as obtained in the C^*M liquid mixture under concentration gradient [12] is also in reasonable agreement with this value (see Fig. 4, where the border data are reported).

Why is there such a well-defined border between a disconnected morphology–slow growth and an interconnected morphology–fast growth? According to Nikolaev, Beysens, and Guenoun [3], two mechanisms are in competition for inducing coalescence: Brownian motion and hydrodynamic interaction. When the volume fraction is small, the droplets are far apart and the only mechanism which brings two droplets into contact for coalescence is Brownian motion. This mechanism was considered by Smoluchowski [20] for coagulation of colloids and then applied to phase separation by Binder and Stauffer [1] and Siggia [2]. The pattern of droplet is made of isolated droplets, whose mean radius or distance grow as $t^{1/3}$. When the volume fraction becomes larger, the flow generated by a first coalescence is able to generate another coalescence between the fusioning drops and its neighbors. This leads to the formation of a new elongated droplet. When the drops are close enough to each other the fusioning drops have no time to go back to a spherical shape since a new coalescence takes place before relaxation. An interconnected pattern naturally follows, whose typical wavelength grows as t^1. The interdroplet distance, measured for monodisperse droplets by the equilibrium volume fraction ϕ of the minority phase, is thus the important parameter. A numerical simulation of a simplified coalescence process predicts a crossover $\phi_H\approx26\%$ [3], a value which compares well with our measurements. These findings have been recently confirmed by a totally different method, involving full three-dimensional simulations of the Boltzmann-Vlasov equations of the phase separating fluid [21].

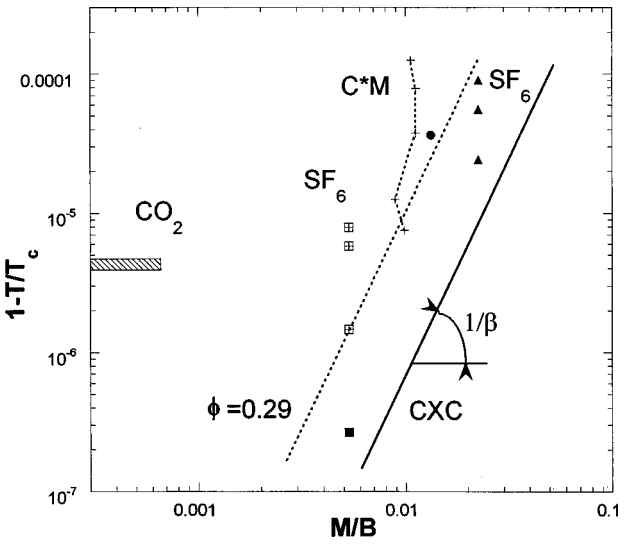

FIG. 4. Reduced coexistence curve ($1-T/T_c$ with respect to M/B in a log-log plot; see text) with the experimental volume fractions and the different growth laws and morphologies. The full line is the coexistence curve ($\phi=0$). The dotted line ($\phi=0.29$) is the estimated boundary between the regions of slow-disconnected and fast-interconnected evolution. The open dots correspond to the interconnected-fast growth and full dots correspond to the disconnected-slow growth. Square: this experiment. Circles and triangles: from Ref. [14]. CO_2 is from Ref. [9]. Crosses correspond to the boundary observed in a binary liquid under concentration gradient [12].

V. CONCLUSION

These results, obtained in the absence of gravity effects, show clearly that, during the phase separation of fluid phases, the volume fraction of the minority phase is the key parameter which governs the hydrodynamic correlation between the domains and thus the morphology and the evolution law of the pattern. It remains to determine, by refining both experiments and theory, a more precise value for the threshold between the ''fast-interconnected'' and ''slow-disconnected'' domains. However, there remains also an open problem concerning the discrepancy between the kinetics of binary liquids and pure fluids that we plan to address in the near future.

ACKNOWLEDGMENTS

We are indebted to C. Chabot for her contribution. The experimental setup has been constructed by MBB ERNO, where ESTEC is the project leader under ESA funding. The CNES has supported the ground-based studies. NASA has provided the flight resources.

[1] K. Binder and D. Stauffer, Phys. Rev. Lett. **33**, 1006 (1974); K. Binder, Solid State Commun. **34**, 191 (1980).
[2] D. Siggia, Phys. Rev. A **20**, 595 (1979).
[3] V. S. Nikolaev, D. Beysens, and P. Guenoun, Phys. Rev. Lett. **76**, 3144 (1996); V. S. Nikolaev and D. Beysens, Phys. Fluids **9**, 3227 (1997).
[4] J. D. Gunton, M. San Miguel, and P. S. Sahni, in *Phase Transitions and Critical Phenomena*, edited by C. Domb and J. L. Lebowitz (Academic, New York, 1983), Vol. 8, p. 269, and references therein.
[5] K. Kawasaki, in *Phase Transitions and Critical Phenomena*, edited by C. Domb and J. L. Lebowitz (Academic, New York, 1976), Vol. 5a, p. 166, and references therein.
[6] H. E. Stanley, *Introduction to Phase Transitions and Critical Phenomena* (Clarendon, Oxford, 1971).
[7] K. Binder, in *Material Science and Technology: Phase Transformations in Materials*, edited by P. Haasen (VCH Verlagsgesellschaft, Weinheim, Germany, 1991), Vol. 5, p. 405, and references therein.
[8] P. Guenoun, R. Gastaud, F. Perrot, and D. Beysens, Phys. Rev. A **36**, 4876 (1987), and references therein.
[9] Y. Garrabos, B. Le Neindre, P. Guenoun, B. Khalil, and D. Beysens, Europhys. Lett. **19**, 491 (1992), and references therein.
[10] H. Furukawa, Adv. Phys. **34**, 703 (1985), and references therein.
[11] N. C. Wong and C. M. Knobler, Phys. Rev. A **24**, 3205 (1981).
[12] Y. Jayalakshmi, B. Khalil, and D. Beysens, Phys. Rev. Lett. **69**, 3088 (1992).
[13] A. Cumming, P. Wiltzius, F. S. Bates, and J. H Rosedale, Phys. Rev. A **45**, 885 (1992); T. Baumberger, F. Perrot, and D. Beysens, *ibid.* **46**, 7636 (1992).
[14] F. Perrot, P. Guenoun, T. Baumberger, D. Beysens, Y. Garrabos, and B. Le Neindre, Phys. Rev. Lett. **73**, 688 (1994).
[15] I. M Lifshitz and V. V. Slyozov, J. Phys. Chem. Solids **19**, 35 (1961).
[16] C. Morteau, M. Salzmann, Y. Garrabos, and D. Beysens, in *Fluids in Space*, edited by A. Viviani (Jean Gilder Congressi srl, Naples, 1996), p. 327.
[17] International Microgravity Laboratory (IML2) onboard the space shuttle (July 1994).
[18] See, e.g., A. Onuki and R. A. Ferrell, Physica A **164**, 245 (1990); P. Guenoun, B. Khalil, D. Beysens, Y. Garrabos, F. Kammoun, B. Le Neindre, and B. Zappoli, Phys. Rev. E **47**, 1531 (1993).
[19] The Critical Point Facility is described in Microgravity News **3**, No. 2, 5 (1990).
[20] M. Von Smoluchowski, Z. Phys. Chem., Stoechiom. Verwandtschaftsl. **92**, 129 (1917).
[21] S. Bastea and J. L. Lebowitz, Phys. Rev. Lett. **78**, 3499 (1997).